Measurement of nuclear effects in neutrino interactions with minimal dependence on neutrino energy

X.-G. Lu,[1,*] L. Pickering,[2] S. Dolan,[1] G. Barr,[1] D. Coplowe,[1] Y. Uchida,[2] D. Wark,[1,3] M. O. Wascko,[2] A. Weber,[1,3] and T. Yuan[4]

[1]*Department of Physics, Oxford University, Oxford, Oxfordshire, United Kingdom*
[2]*Department of Physics, Imperial College London, London, United Kingdom*
[3]*STFC Rutherford Appleton Laboratory, Harwell Oxford, Oxfordshire, United Kingdom*
[4]*Department of Physics, University of Colorado Boulder, Boulder, Colorado 80309, USA*

(Received 17 December 2015; revised manuscript received 27 June 2016; published 28 July 2016)

We present a phenomenological study of nuclear effects in neutrino charged-current interactions, using transverse kinematic imbalances in exclusive measurements. Novel observables with minimal dependence on neutrino energy are proposed to study quasielastic scattering and especially resonance production. They should be able to provide direct constraints on nuclear effects in neutrino- and antineutrino-nucleus interactions.

DOI: 10.1103/PhysRevC.94.015503

I. INTRODUCTION

The study of neutrino interactions presents unique challenges. Unlike for its electroweak counterpart, the charged lepton, the energy of a neutrino is generally difficult to measure. Existing accelerator technologies are able to provide a neutrino beam with a well-defined direction, and yet the beam energy spectrum, which is of critical importance in neutrino oscillation analyses [1,2], is not well known. With a nuclear target, where neutrinos interact with bound nucleons, uncertainties from various nuclear effects arise. With accelerator neutrinos in the GeV regime, individual bound nucleons are resolved. Their momenta, due to Fermi motion ranging up to $p_{\mathrm{F}} \sim 200\,\mathrm{MeV}/c$, need to be considered; the energy required to release one of them (binding energy) causes further fluctuations in the initial kinematics. Moreover, multinucleon correlations have recently been conjectured to contribute significantly to the measured cross sections in this energy regime, evoking a reexamination of the long-used impulse approximation [3,4]. Because the hadronic final states are produced inside a nuclear medium—the nucleus containing nucleons undergoing Fermi motion—they experience final-state interactions (FSIs) before exiting and therefore both their kinematics and identity can be altered. In response to this, the nucleus can be excited or it can break up, emitting nucleons, pions, and photons—collectively known as *nuclear emission*. These effects further modify the final states from the *basic* neutrino-nucleon interaction, which could have already been biased by multinucleon correlations, and introduce ambiguities, in both measurements and calculation, to efforts to identify the interaction channel. The highly convoluted nature of the problem is made manifest by the fact that these nuclear effects are all present in different channels for all nuclei except hydrogen [5].

Experimental efforts to understand charged-current (CC) neutrino-nucleus interactions, on which spectrum measurements of accelerator neutrinos are based, have been focused on inclusive and semi-inclusive observables, such as total cross sections and lepton kinematics, which depend strongly on the neutrino energy and cannot be directly compared across experiments because the neutrinos are produced in wideband fluxes. To interpret the data, theories of the basic interactions and nuclear effects have to be folded into approximated neutrino energy spectra. Therefore, on one hand, accessing the nuclear effects precisely is difficult, while on the other hand, understanding the nuclear effects helps determine the spectra. For example, Ref. [5] shows that, with moderate FSIs, the calorimetric approach of neutrino energy reconstruction outperforms kinematic methods; yet models of FSIs have not been extensively tested because of the lack of measurements of the final-state hadrons.

In this work, we propose to measure nuclear effects via the transverse kinematic imbalance between the charged lepton and the primary final-state hadron in an exclusive CC channel, such as quasielastic scattering (QE) and resonance production (RES). The measurement in RES is especially important for a better understanding of nuclear effects in both neutrino and antineutrino interactions. Our discussion starts with the impulse approximation. We first demonstrate the minimal dependence of hadronic variables on the neutrino energy and describe the nuclear medium response to FSIs. Then we illustrate how these variables are affected by Fermi motion and FSIs. Subsequently the issue with respect to multinucleon correlations and an extension of the technique to electron-nucleus scattering are addressed briefly.

II. NUCLEAR MEDIUM RESPONSE

Consider a CC interaction on a nucleus. At the basic level the neutrino ν interacts with a bound nucleon N that then transits to another hadronic state N':

$$\nu + N \rightarrow \ell' + N', \tag{1}$$

where ℓ' is the charged lepton. In the rest frame of the nucleus, the bound nucleon is subject to Fermi motion with momentum $\vec{p}_N$, and an energy-momentum $(\omega,\vec{q})$ carried by a virtual W boson (W^*) is transferred to it as the neutrino scatters. In

*xianguo.lu@physics.ox.ac.uk

characterizing the interaction, the virtuality $Q^2 \equiv q^2 - \omega^2$ and the invariant mass W of N' are used. Following energy-momentum conservation (the binding energy is neglected compared to the initial nucleon energy[1]), the energy transfer reads

$$\omega = \frac{Q^2 + W^2 - m_N^2 + 2\vec{q}\cdot\vec{p}_N}{2\sqrt{m_N^2 + p_N^2}}, \tag{2}$$

$$\sim \frac{Q^2 + W^2 - m_N^2}{2\sqrt{m_N^2 + p_N^2}}, \tag{3}$$

where m_N is the mass of N and the last line follows from averaging out the direction of $\vec{p}_N$ in Eq. (2), which is a first-order approximation because the *polarization* term $\vec{q}\cdot\vec{p}_N$ with opposite orientations of $\vec{p}_N$ for a given $\vec{q}$ does not exactly cancel—the W^*-N cross section is slightly different with the varying center-of-mass energy.[2] Below the deeply inelastic scattering region—especially in QE and RES where W equals the nucleon and dominantly the $\Delta(1232)$ resonance mass, respectively—the cross section is suppressed when Q is larger than the nucleon mass. The hadron momentum in these channels, as indicated by Eq. (3), "saturates" if the neutrino energy is above the scale $Q^2/2m_N \sim \mathcal{O}(0.5\ \text{GeV})$, beyond which the charged lepton retains most of the increase of the neutrino energy.

Once the final-state hadron N' is produced, it starts to propagate through the nuclear medium.[3] Under the assumption that the basic interaction [Eq. (1)] and the in-medium propagation are uncorrelated (i.e., are *factorized*), the momentum of N', which depends weakly on the neutrino energy, completely determines the medium response, including the in-medium interaction probability τ_f [4] and the energy-momentum transfer $(\Delta E, \Delta\vec{p})$ to the medium (if N' decays inside the nucleus, the total effect of all decay products is considered). It is the latter that leads to nuclear excitation[5] or break-up and consequently nuclear emission. The nuclear emission probability, $P(\Delta E, \Delta\vec{p})$, correlates the medium response to the in-medium energy-momentum transfer.[6] The factorization assumption suggests that $P(\Delta E, \Delta\vec{p})$ is independent of the neutrino energy

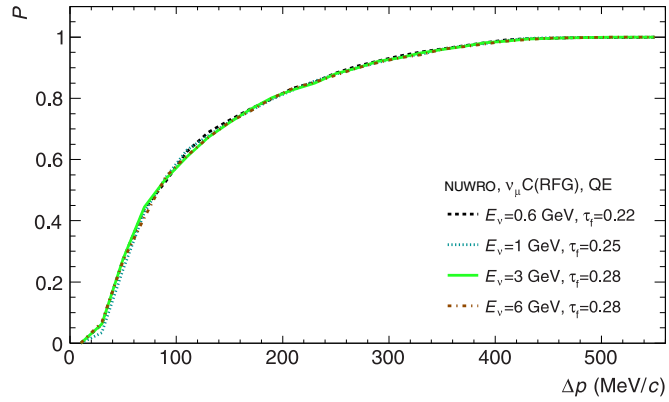

FIG. 1. Nuclear emission probability as a function of the in-medium momentum transfer, simulated by NUWRO [6] for ν_μ CC QE on carbon—nuclear state modeled as relativistic Fermi gas (RFG) [7]—at a neutrino energy of 0.6, 1, 3, and 6 GeV. Multinucleon correlations are ignored. The in-medium interaction probability τ_f (extracted from the simulation output throughout this work) is shown in the legend.

E_ν, which is consistent with the implementation in the NUWRO[7] [6] simulation shown in Fig. 1. In addition, as the neutrino energy increases, the predicted FSI strength saturates, as is indicated by τ_f in the figure.

III. SINGLE-TRANSVERSE KINEMATIC IMBALANCE

To make a neutrino energy-independent measurement of nuclear effects, the in-medium energy-momentum transfer $(\Delta E, \Delta\vec{p})$ would be the ideal observable; this however is not experimentally accessible because of the unknown initial nucleon momentum and the initially unknown neutrino energy. Instead, $\Delta\vec{p}$ can be directly inferred from the following single-transverse kinematic imbalance (Fig. 2):

$$\delta\vec{p}_T \equiv \vec{p}_T^{\,\ell'} + \vec{p}_T^{\,N'}, \tag{4}$$

$$\delta\alpha_T \equiv \arccos\frac{-\vec{p}_T^{\,\ell'}\cdot\delta\vec{p}_T}{p_T^{\ell'}\delta p_T}, \tag{5}$$

where $\vec{p}_T^{\,\ell'}$ and $\vec{p}_T^{\,N'}$ are the projections of the extra-nucleus final-state momenta transverse to the neutrino direction. In particular, $-\vec{p}_T^{\,\ell'} = \vec{q}_T$, the transverse component of $\vec{q}$.

If the initial-state nucleon were static and free, δp_T would be 0—a feature that is not possessed by other experimentally accessible variables such as the final-state momenta. If FSIs could be switched off, $\delta\vec{p}_T$ and $\delta\alpha_T$ would be the transverse projection of $\vec{p}_N$ and of the angle between $\vec{p}_N$ and $\vec{q}$, respectively. Accordingly, to first approximation, the distribution of $\delta\vec{p}_T$ would be independent of the neutrino energy and that of $\delta\alpha_T$ would be flat due to the isotropy of Fermi motion. The FSI acceleration (deceleration) of the propagating N' adds in a

[1]The full form with the intranucleus potential will modify the apparent mass and the relativistic energy-momentum conversion of the initial nucleon.

[2]The bias to the mean ω is about 1% in a NUWRO estimation (for technical detail see caption of Fig. 1).

[3]The exclusive measurement discussed in this work is not sensitive to the absorption and charge exchange in FSIs, and therefore these effects are not considered.

[4]The in-medium interaction probability is a functional of the nucleon momentum distribution in the nucleus.

[5]For simplicity, the nucleus excitation during the basic interaction is not discussed here.

[6]To be precise, the nuclear emission considered here is from the deexcitation within a detection time window. In practice, slow emission with a longer transition time is effectively seen as no emission. Another way the in-medium energy-momentum transfer is carried away is via the nucleus recoil.

[7]Conclusions in this work are independent of the chosen generator for demonstration.

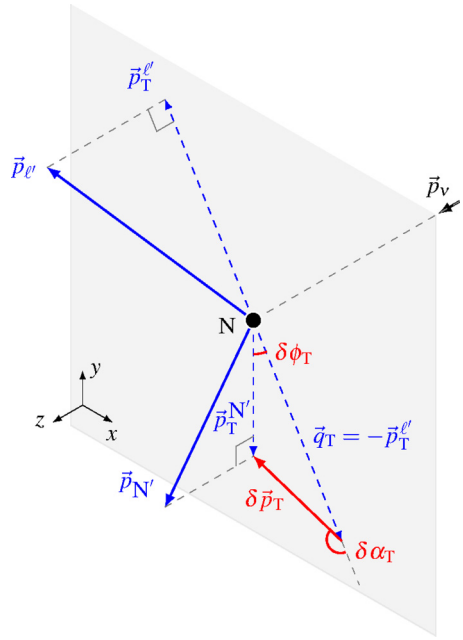

FIG. 2. Schematic illustration of the single-transverse kinematic imbalance—$\delta\phi_T$, $\delta\vec{p}_T$, and $\delta\alpha_T$—defined in the plane transverse to the neutrino direction.

smearing to δp_T and pushes $\delta\vec{p}_T$ forward (backward) to $(-)\vec{q}_T$, making $\delta\alpha_T \to 0^\circ$ (180°).

Second-order effects that lead to the dependence on the neutrino energy include the previously discussed polarization [see text after Eq. (2)], Pauli blocking, and the transverse projection. The combined effect determines the evolution of the $\delta\alpha_T$ distribution with $p_T^{\ell'}$. An example predicted by NUWRO is shown in Fig. 3. At $p_T^{\ell'} \lesssim p_F$, the cross section for $\delta\alpha_T$ at 180° is suppressed in QE interactions due to Pauli blocking, which leads to a forward peak in the distribution of $\delta\alpha_T$ at small $p_T^{\ell'}$. As $p_T^{\ell'} \to E_\nu$, the cross section for $\delta\alpha_T$ at 0° is suppressed by the conservation of the longitudinal momentum.

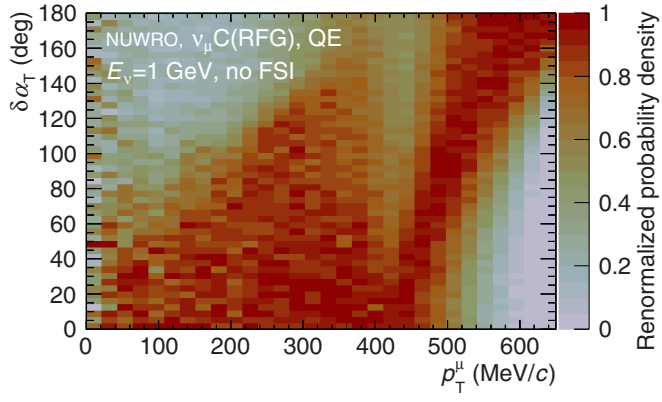

FIG. 3. Conditional probability density function of $\delta\alpha_T$ as a function of the muon p_T without FSIs (each slice of p_T^μ is normalized in such a way that the maximum is 1; the renormalized density is shown on the z axis), predicted by NUWRO for ν_μ CC QE on carbon (RFG) at a neutrino energy of 1 GeV with FSIs switched off.

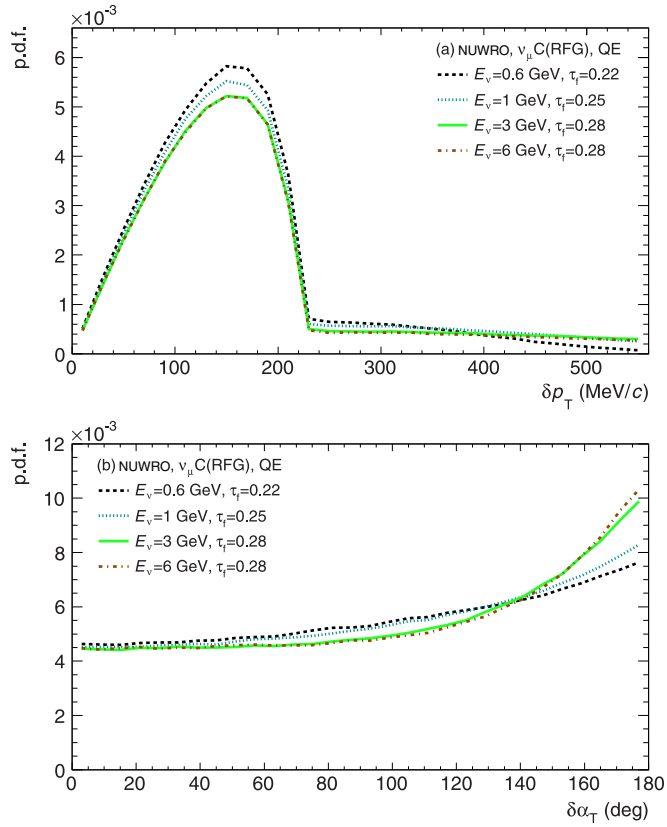

FIG. 4. Probability density function of δp_T (upper) and $\delta\alpha_T$ (lower) predicted by NUWRO for different neutrino energies.

Even though the fractions of events in both extremes of the $p_T^{\ell'}$ spectrum change with the neutrino energy, they are insignificant for the few GeV neutrino interactions. As a result, the δp_T and $\delta\alpha_T$ distributions are largely independent of E_ν, as is shown in Fig. 4, where the evolution of the distributions with the neutrino energy is dominated by variations in the FSI strength.

The transverse momentum imbalance δp_T has been used by the NOMAD experiment to enhance the purity of the selected QE [8], while the "transverse boosting angle" $\delta\alpha_T$ is proposed here for the first time. Experimental data on $\delta\alpha_T$ will reveal the accelerating and decelerating nature of FSIs. Its dependence on $p_T^{\ell'}$, measured in a detector that has a low momentum threshold, will additionally provide constraints on Pauli blocking.

Besides the transverse momentum imbalance and boosting angle, another single-transverse variable can be defined (Fig. 2):

$$\delta\phi_T \equiv \arccos\frac{-\vec{p}_T^{\,\ell'}\cdot\vec{p}_T^{\,N'}}{p_T^{\ell'}\,p_T^{N'}}, \tag{6}$$

which measures the deflection of N' with respect to $\vec{q}$ in the transverse plane. If the initial-state nucleon were static and free, $\delta\phi_T$ would be 0; with nuclear effects, the deflection caused by $\Delta\vec{p}$ adds in a smearing to the initial distribution of $\delta\phi_T$ that is determined by $\vec{p}_N$. Experiments have measured the $\delta\phi_T$ distribution in QE-like events [9] and used it to enhance the QE purity [8,10]. However, the trigonometric

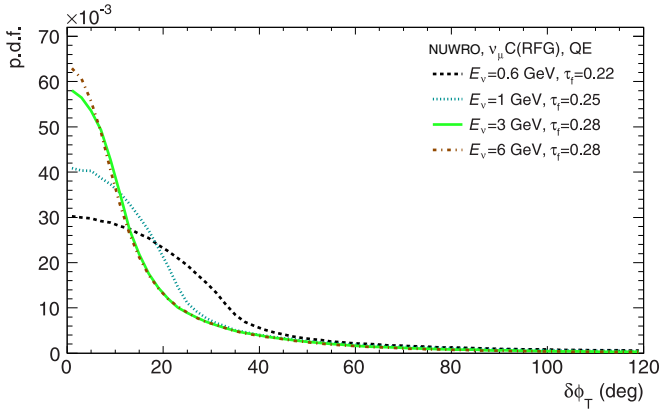

FIG. 5. Probability density function of $\delta\phi_T$.

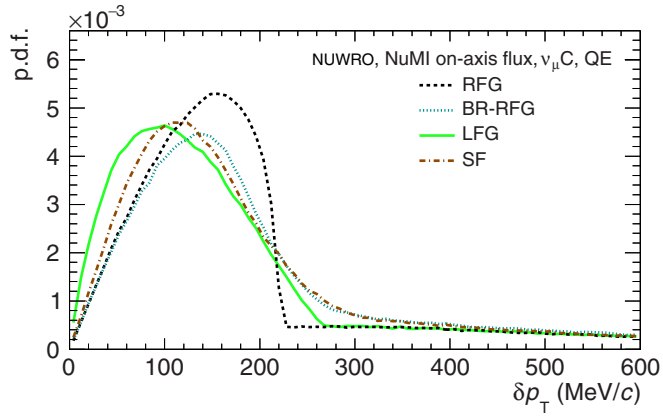

FIG. 6. NUWRO predictions for δp_T with different nuclear states: relativistic Fermi gas (RFG) [7], relativistic Fermi gas with the Bodek-Ritchie modifications (BR-RFG) [13], local Fermi gas (LFG) [14], and spectral function (SF) [15]. The NuMI [11] on-axis flux shape is used to simulate the neutrino energy distribution.

relation illustrated by Fig. 2 shows that $\delta\phi_T$ scales with $\delta p_T/p_T^{\ell'}$ and therefore depends on the lepton kinematics which are sensitive to the neutrino energy. The energy dependence of $p_T^{\ell'}$ counteracts the FSI deflection and the uncertainties from the nuclear effects and neutrino flux become convolved. The distribution of $\delta\phi_T$ by NUWRO is shown in Fig. 5 for different neutrino energies. In contrast to the expected evolution with the FSI strength, the distribution becomes narrower at higher energy because of the increase of $p_T^{\ell'}$. This serves as an example of how the neutrino energy dependence can bias a measurement of nuclear effects. Because of the $p_T^{\ell'}$ dependence, the single-transverse variables all suffer to some extent from a dependence on the neutrino energy even after kinematic saturation is reached. Nevertheless, the study of nuclear effects can be performed by restricting $p_T^{\ell'}$.

IV. MODEL PREDICTIONS

In the previous discussion, an equivalence is established between the nuclear effects in neutrino-nucleus interactions and the transverse kinematic imbalance. Initial- and final-state effects can be directly observed via $\delta\vec{p}_T$, as can be seen by rewriting Eq. (4) as

$$\delta\vec{p}_T = \vec{p}_T^{\,N} - \Delta\vec{p}_T, \tag{7}$$

where $\vec{p}_N$ is the momentum of the initial nucleon. In this section we present the latest predictions of the single-transverse variables. Interactions of neutrinos from the NuMI (on-axis) beam line [11] on a carbon target are simulated by NUWRO (Version 11q) [6] and GENIE (Version 2.10.0) with the hA FSI model [12]. Because the neutrino energy is well above the saturation scale $\mathcal{O}(0.5$ GeV), the minimal energy dependence of the transverse kinematic imbalance applies. Interesting features of the implemented nuclear effects in the models are therefore maximally preserved and readily identified as shown below.

The NUWRO prediction for δp_T in QE is shown in Fig. 6. Four models of the nuclear state—relativistic Fermi gas (RFG) [7], relativistic Fermi gas with the Bodek-Ritchie modifications (BR-RFG) [13], local Fermi gas (LFG) [14], and spectral function (SF) [15]—are compared. The deformation of the p_T^N shape due to FSIs, which results in the long tail towards the upper end of the δp_T distribution, is limited by the FSI strength quantified by τ_f. For finite τ_f, as is the case predicted by NUWRO (see, e.g., Fig. 1), the δp_T shapes largely preserve the Fermi motion distributions—a useful technique for understanding novel target materials in future experiments such as DUNE [1].

The NUWRO and GENIE predictions for $\delta\alpha_T$ and $\delta\phi_T$ in QE are shown in Fig. 7. When FSIs are switched off in both simulations, consistent distributions are observed. With the nominal settings, the two predictions significantly differ in the $\vec{q}_T$-collinear regions—$\delta\alpha_T \sim 0^\circ$ and 180° and $\delta\phi_T \sim 0^\circ$—where GENIE predicts a much enhanced probability. While the NUWRO distributions show *normal* evolution when FSIs are switched on as one would expect from the in-medium deflection and deceleration caused by FSIs, the GENIE distributions show an *inverted* tendency. Motivated by this observation, the GENIE Collaboration suggested the effect of the *elastic interaction* of the hA FSI model be investigated. In the nominal GENIE simulation for QE on carbon, events with protons that undergo this FSI interaction amount to about 40% at the NuMI beam energy. After removing these events, the GENIE prediction is more consistent with the NUWRO nominal one, as is shown in Fig. 7. Further investigation taking into account the dependence on $p_T^{\ell'}$ (in an approach similar to that of Fig. 3) shows that in $\delta\alpha_T$ the collinear enhancement is of an apparent acceleration feature at low q_T ($\lesssim$200 MeV/c at NuMI energy) and deceleration at high q_T.

V. DISCUSSION

The definitions of the transverse kinematic imbalance require an exclusive measurement of the primary final-state particles. In RES, the imbalance is defined between the charged lepton and the $p\pi^{+(-)}$ system with a ν ($\bar{\nu}$) beam. Transverse kinematic imbalance in RES, proposed for the first time, should provide information on the resonance and pion FSIs. As an example, the NUWRO and GENIE predictions for δp_T in Δ^{++} ($p\pi^+$) production are shown in Fig. 8. In the NUWRO

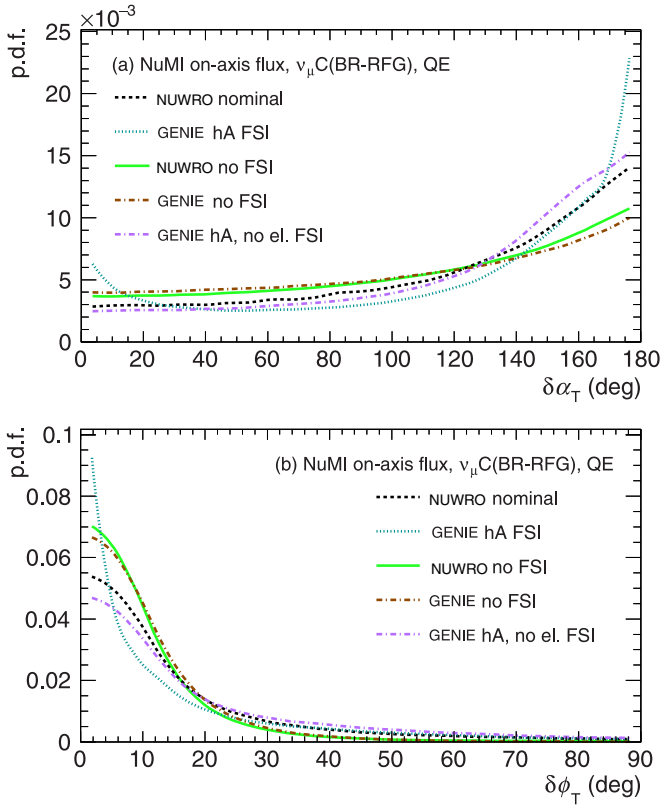

FIG. 7. NUWRO and GENIE predictions for $\delta\alpha_T$ (upper) and $\delta\phi_T$ (lower). Nominal distributions are compared to the cases where FSIs are disabled. Further comparison is made by removing nominal GENIE events that experienced proton elastic FSIs (see text for exact definition).

predictions, the deformation of the p_T^N shape is more severe in RES than in QE because of the additional FSIs from the pion final state; for GENIE, both the proton and pion hA elastic interactions contribute to an *inverted* deformation of the p_T^N shape towards the lower end of the δp_T distribution. Because all simulations use the same nuclear state (BR-RFG), stronger FSIs in GENIE can be inferred by its more pronounced upper tail in the distribution.

Another interesting example from the transverse kinematic imbalance in RES is the Pauli blocking of the resonance decay product. If it does not affect the resonance momentum—this is expected because the polarization of the decay product alone can vary to fulfill Pauli blocking—the $\delta\alpha_T$ distribution at small $p_T^{\ell'}$ ($\lesssim p_F$) will not be suppressed at 180°, different from the QE case.

So far the discussion only considers the in-medium energy-momentum transfer and nuclear emission that are induced by FSIs. In reality, multinucleon correlations in the initial

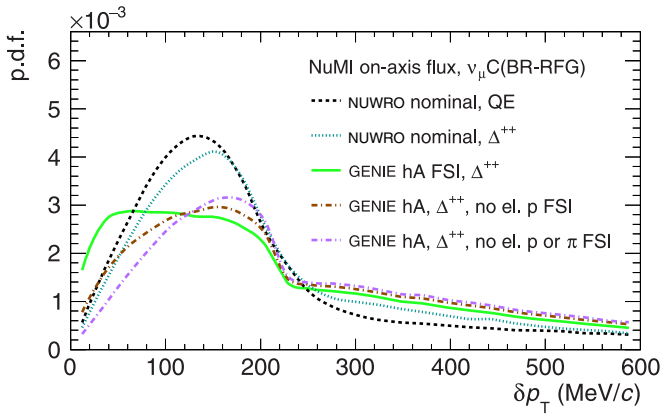

FIG. 8. NUWRO and GENIE predictions for δp_T in QE and Δ^{++} ($p\pi^+$) production. Nominal GENIE events that experienced proton and pion elastic FSIs were removed stepwise to separate the effects; similar features are also exhibited in the $p\pi^-$ and $p\pi^0$ channels.

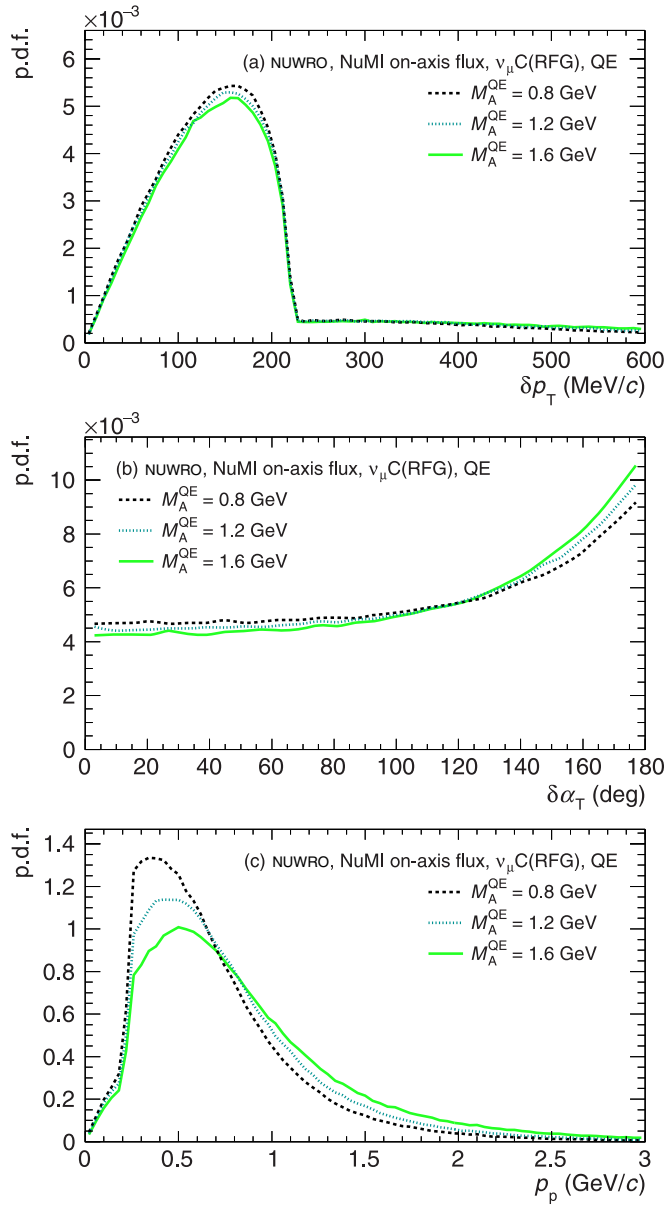

FIG. 9. Comparison of δp_T (a), $\delta\alpha_T$ (b), and the final-state proton momentum p_p (c) in QE for different values of the axial mass M_A^{QE}: 0.8, 1.2 (nominal), and 1.6 GeV. It shows that the transverse kinematic imbalances are much less sensitive to the variation of M_A^{QE}.

state could have significant impact in both processes that are however indistinguishable from being FSI-induced on an event-by-event basis. Their contribution to the kinematic imbalance results in an additional convolution to each of the single-transverse variables. The δp_T and $\delta\alpha_T$ distributions—especially in the regions beyond the Fermi momentum and around the backward peak, respectively—may therefore provide a kinematic constraint on the multinucleon correlations. Furthermore, because the nuclear emission probability is enhanced, its correlations against the single-transverse variables may be of interest to provide sensitive signatures.

In general, samples of QE and RES can be produced by selecting events with at least one proton and no pion and at least one proton and one pion, respectively, in a CC inclusive sample. Neutrino energy-dependent contamination comes from other channels where incomplete final states are selected. In addition, because of their intrinsic kinematic imbalance, such nonexclusive backgrounds mimic the exclusive signals that experience FSIs and/or multinucleon correlations. However, quantitatively they may behavior differently: because of the characteristic strengths of the imbalance, one would expect that the single-transverse variables from the background, the signal with FSIs, and that with multinucleon correlations form a certain ordering, based on which it might be possible to perform efficient channel purification and nuclear effect identification.

The observation of the transverse kinematic imbalance relies on the momentum reconstruction of both leptonic and hadronic final states. Because the $\delta\vec{p}_T$ distributions reveal nuclear effects including Fermi motion, FSI deflection, acceleration, and deceleration, efforts to improve the momentum and angular resolution, as well as to understand the momentum scales of the final-state lepton, proton, and pion, might be needed for current experiments. Experiments with trackers, for example T2K [16] and MINERvA [17], might be capable to perform pioneering measurements to validate the different model predictions presented in the previous section. The prospect in MINERvA with its multiple-type nuclear targets is of special interest because the transverse kinematic imbalance would directly show the evolution of the nuclear effects as the target type varies.

Throughout this work, it is emphasized that the equivalence between nuclear effects and transverse kinematic imbalance is invariant with the neutrino energy. In fact this equivalence is invariant with *all* physics at the neutrino-nucleon interaction level. In analogy to the minimal neutrino energy dependence, transverse kinematic imbalances are also minimally influenced by nucleon level model uncertainties, such as the details of the nucleon form factors (Fig. 9). This further reduces the uncertainties in measuring nuclear effects.

Even though this work is intended for neutrino interactions, the technique can be used in electron-nucleus scattering to probe nuclear effects in general. In such a case, because the electron beam energy is well known, the energy imbalance between the initial and final states can also be studied.

VI. SUMMARY

In this work, for measurement of nuclear effects independent of the neutrino energy, transverse kinematic imbalance has been systematically examined. Its novel application to the resonance production is important for experiments with high energy neutrinos produced in the NuMI and LBNF [1] beam lines because of the significant production cross section; it is also unique for the study of nuclear effects in antineutrino interactions where the final-state neutrons in quasielastic scattering cannot usually be measured. An extension of the single-transverse kinematics in the resonance production is the double-transverse momentum imbalance [5,18], which is defined on the axis perpendicular to both the neutrino and the charged lepton momenta, with a sensitivity to the difference between the proton and pion FSIs. A comprehensive description of nuclear effects in neutrino interactions should be attainable from future measurements of the single- and double-transverse kinematic imbalance on various nuclear targets in different interaction channels.

ACKNOWLEDGMENTS

The authors express their gratitude to the NuWro and GENIE Collaborations for the helpful discussions about using the generators in this work and to K. Duffy, S. Dytman, Y. Hayato, K. McFarland, R. Shah, J. Sobczyk, T. Stewart, and C. Wilkinson for helpful discussions. This work is supported by the UK Science and Technology Facilities Council and (T.Y.) by the DOE and the DOE Early Career program, USA.

[1] C. Adams *et al.* (LBNE Collaboration), Report Nos. BNL-101354-2013-JA, BNL-101354-2014-JA, FERMILAB-PUB-14-022, LA-UR-14-20881 (2013) [arXiv:1307.7335].
[2] K. Abe *et al.* (Hyper-Kamiokande Proto-Collaboration), Prog. Theor. Exp. Phys. **2015**, 053C02 (2015).
[3] M. Martini, M. Ericson, G. Chanfray, and J. Marteau, Phys. Rev. C **81**, 045502 (2010).
[4] J. Nieves, I. Ruiz Simo, and M. J. Vicente Vacas, Phys. Lett. B **707**, 72 (2012).
[5] X.-G. Lu, D. Coplowe, R. Shah, G. Barr, D. Wark, and A. Weber, Phys. Rev. D **92**, 051302 (2015).
[6] T. Golan, C. Juszczak, and J. T. Sobczyk, Phys. Rev. C **86**, 015505 (2012).
[7] E. J. Moniz, Phys. Rev. **184**, 1154 (1969).
[8] V. Lyubushkin *et al.* (NOMAD Collaboration), Eur. Phys. J. C **63**, 355 (2009).
[9] T. Walton *et al.* (MINERvA Collaboration), Phys. Rev. D **91**, 071301 (2015).

[10] K. Abe *et al.* (T2K Collaboration), Phys. Rev. D **91**, 112002 (2015).
[11] K. Anderson *et al.*, Tech. Rep. No. FERMILAB-DESIGN-1998-01, http://lss.fnal.gov/archive/design/fermilab-design-1998-01.shtml.
[12] C. Andreopoulos *et al.*, Nucl. Instrum. Methods Phys. Res., Sect. A **614**, 87 (2010).
[13] A. Bodek and J. L. Ritchie, Phys. Rev. D **23**, 1070 (1981).
[14] T. Leitner, O. Buss, L. Alvarez-Ruso, and U. Mosel, Phys. Rev. C **79**, 034601 (2009).
[15] O. Benhar, D. Day, and I. Sick, Rev. Mod. Phys. **80**, 189 (2008).
[16] K. Abe *et al.* (T2K Collaboration), Nucl. Instrum. Methods Phys. Res., Sect. A **659**, 106 (2011).
[17] L. Aliaga *et al.* (MINERvA Collaboration), Nucl. Instrum. Methods Phys. Res., Sect. A **743**, 130 (2014).
[18] X.-G. Lu, arXiv:1512.09042.